Gait Based on the Spring-Loaded Inverted Pendulum

Hartmut Geyer and Uluc Saranli

Contents

1 Introduction . . . 2
  1.1 Biomechanical Foundation . . . 2
  1.2 Adoption in Robotics . . . 4
2 Legged Platforms Inspired by the SLIP Model . . . 5
3 Planar SLIP Dynamics and Control Methods . . . 8
  3.1 Model Formulation . . . 8
  3.2 Return Map Analysis of Model Dynamics . . . 9
  3.3 Approximate Solutions to SLIP Dynamics . . . 11
  3.4 Intuitive Control Strategies . . . 12
  3.5 SLIP Control Derived from Return Maps . . . 14
4 Generalizations . . . 17
  4.1 Multistep Planning . . . 17
  4.2 Running in 3-D Environments . . . 17
  4.3 Walking and Gait Transitions . . . 18
  4.4 Embedding in Humanoids and Other Legged Robots . . . 20
5 Future Directions and Open Problems . . . 22
References . . . 22

Abstract

The spring-loaded inverted pendulum (SLIP) describes gait with a point mass rebounding on spring legs. The model captures the center of mass dynamics observed in running animals and has become a basic gait template in biome-

H. Geyer (✉)
Robotics Institute, Carnegie Mellon University, Pittsburgh, PA, USA
e-mail: hgeyer@cs.cmu.edu

U. Saranli
Department of Computer Engineering, Middle East Technical University, Balgat, Ankara, Turkey
e-mail: saranli@ceng.metu.edu.tr

A. Goswami, P. Vadakkepat (eds.), *Humanoid Robotics: A Reference*,
https://doi.org/10.1007/978-94-007-7194-9_43-1

chanics and robotics for studying the dynamics and control of compliant legged locomotion. This chapter provides an overview of gait based on the SLIP model. The standard SLIP model for describing sagittal plane locomotion is introduced through a review of early model developments in the biomechanics and robotics communities. Related legged platforms are presented. Methods are then discussed for studying the dynamics and control of locomotion with this model, including approximate solutions to the stance dynamics, return map analysis of periodic gait, and optimal control approaches for getting stable and robust running behavior. Finally, generalizations of the SLIP model and its analysis methods are highlighted for performing multistep planning, expanding to locomotion in 3-D environments, generating walking and gait transitions, and embedding in humanoids and other legged robots. The chapter closes with suggestions for future directions that will likely help to grow the utility of the SLIP model as a gait template for agile, stable, and robust locomotion on compliant legs.

Keywords

Spring-loaded inverted pendulum (SLIP) · Spring mass model · Walking · Running · Gait transition · Running robots · Poincare · Return map · Virtual leg control

1 Introduction

The spring-loaded inverted pendulum (SLIP) is a conceptual model for locomotion on compliant legs, originating from the study of running gaits in animals. In the simplest form, it reduces the body to a point mass that rebounds on a massless spring leg in stance and moves on a ballistic trajectory in flight (Fig. 1a). The model combines mathematical simplicity with the ability to capture the translational dynamics (indicated by ground reaction forces in Fig. 1b) of running animals, including humans. As a result, the model has evolved into a standard tool for studying biological control strategies and establishing a mathematical theory of legged locomotion on compliant legs. It also serves as a natural starting point for the design and control of running robots.

1.1 Biomechanical Foundation

The SLIP model has its origin in biomechanics. Although early suggestions about the importance of compliant leg behavior in running date back centuries, quantitative support for this hypothesis emerged only about 50 years ago from biomechanical experiments. Cavagna and colleagues [12] used force plate measurements to calculate the mechanical work performed in human running. They found that the mechanical efficiency of human running requires a substantial contribution of elastic storage and recoil in the musculoskeletal system. This calculation and the

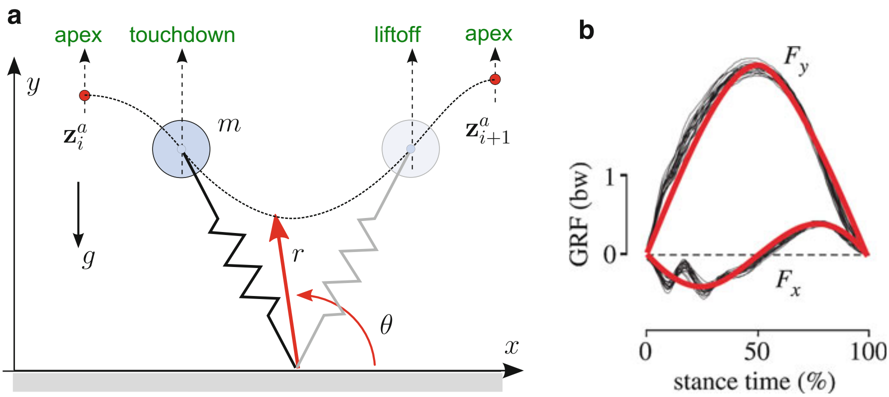

Fig. 1 SLIP model for running gaits. (**a**) A point mass m rebounds on a massless spring with stiffness k and rest length r_0 in stance while moving under the sole influence of gravity (g) in flight. Stance begins when the point mass satisfies a landing condition in flight ($y = r_{td} \sin \theta_{td}$ in this example, where θ_{td} is an assumed angle of attack of the leg). Stance ends when the spring has rebounded to its rest length. (**b**) The model (*red*) reproduces the dominant features of ground reaction forces observed in animal and human running experiments (*black traces*)

observation that the gravitational potential energy and the external kinetic energy of the body's center of mass (CoM) fluctuate in phase during running led them to liken this gait to the behavior of a bouncing rubber ball. The conclusions drawn for humans were found in later studies to extend to hopping and running animals as well, ranging from kangaroos and spring hares to turkeys and rheas and to dogs and rams. Thus, elastic rebound was established as a general concept in animal and human running gaits.

Mathematical models built on this concept followed soon after. McMahon and Greene [39] introduced the rack and pinion model of the leg behavior to study the influence of track stiffness on human running performance. The model represented the vertical leg behavior with a spring (k_m) and dashpot (b) (Fig. 2a). McMahon and Greene used it to calculate the influence of track stiffness (k_t) on the time that runners (mass m) spend in ground contact (2b). The model predicted that there is an intermediate track stiffness at which shorter contact times can be achieved than on hard running surfaces common at that time. The prediction led to installments of tracks with tuned stiffness at Harvard University and Madison Square Garden in New York, which yielded new records at indoor track competitions [39]. Later, McMahon and colleagues [40] reduced the model to an explicit spring and mass system of vertical motion during stance (Fig. 2c), which they used to predict rebound times and vertical ground reactions forces of running animals and humans.

At about the same time, this vertical SLIP model was put to use for studying animal running, and the next step in model formulation took place. In a 1986 workshop on mobile robotics, Blickhan [8] presented the planar version of the SLIP model (Fig. 2c). The planar model explained mechanics of animal running that the vertical model could not capture as it neglects the centrifugal force contribution to

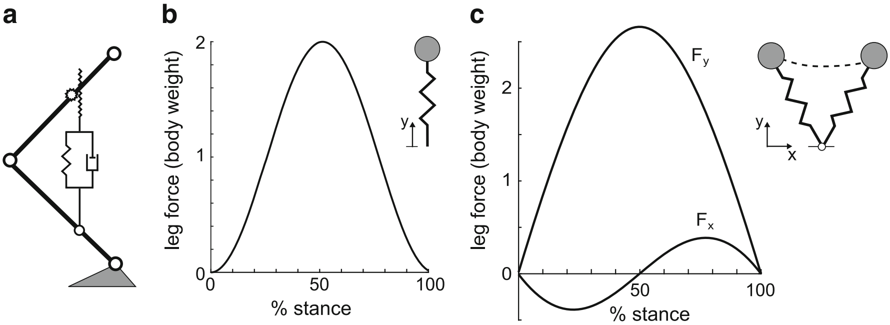

Fig. 2 Early evolution of the SLIP model for running. (**a**) Vertical rack and pinion model of the leg dynamics introduced by McMahon and Greene [39]. (**b**) Vertical SLIP model used by McMahon et al. [40] with example of its ground reaction force. (**c**) Planar version introduced by Blickhan [8] with vertical and horizontal ground reaction forces shown

the rebound dynamics. These key mechanics included the patterns of the horizontal as well as the vertical ground reaction force during running. McMahon and Cheng [38] used the same planar model to predict how stride length and leg excursion angles change with speed in running vertebrates. Subsequent biomechanical studies confirmed and generalized the planar SLIP model's utility in capturing running behavior in humans [16] and in a surprisingly wide variety of other animals [9], triggering further research in the biomechanics community along two main directions: How do animals and humans generate springlike, elastic behavior at the musculoskeletal and neural control levels? And what advantages does this common behavior bring about for (biological) legged systems?

1.2 Adoption in Robotics

For roboticists interested in understanding and recreating animal gait with legged machines, the biomechanical findings about elastic behavior in running animals and humans provided strong incentives to study spring leg robots. As a consequence, they started, somewhat in parallel to the biomechanics community, to explore running with SLIP-type models. Their focus lay, however, on gait stability and control.

In the late 1970s, Raibert had learned from Bizzi about the importance of the springy characteristics of muscles and tendons in the control of animal limb movements and embarked with the development of a computer-controlled pogo stick robot on a long and prolific carrier studying legged locomotion and robots [45]. Although the pogo stick robot was a more complicated machine, the model studied by Raibert and his colleagues to test gait control in simulation included main features of the planar SLIP (Fig. 3a), and they later analyzed the planar SLIP system more explicitly to better predict foot placements for symmetric stance phases of the machine [45].

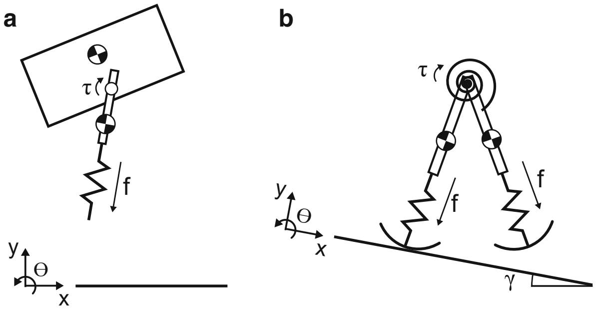

Fig. 3 Early adoption of the SLIP model in robotics. (**a**) Planar hopper model with spring legs used to test running control algorithms for the Raibert hopper [45]. (**b**) Bipedal runner model of McGeer [36] for studying running stability

The first formal study that analyzed running stability with a version of the SLIP model was presented by McGeer [36]. Interested, like Raibert, in building legged machines, McGeer incorporated spring leg behavior into a more realistic biped model whose legs had mass and inertia and were connected at the hip by a torsional spring (Fig. 3b). He analyzed the stride function of this model and predicted mechanical design parameters that lead to periodic running motions. Some of these motions were passively stable. For others, he showed that they could be stabilized with an LQR-derived, active feedback control on leg thrust.

Since these early adoptions, the SLIP model has evolved into the main template for the design and control of running robots. Some legged robots are direct instantiations of the model. Many others actively embed spring – mass behavior using control. In either case, the agility, stability, and robustness of these machines are tied to the agility, stability, and robustness of the underlying model, propelling active research in dynamics and control of legged locomotion based on this template.

2 Legged Platforms Inspired by the SLIP Model

Legged robot platforms inspired by the SLIP model range from mechanical designs that directly embody the model to higher degree of freedom platforms that seek to embed SLIP behavior by active control.

The Raibert hopper was the first legged robot that directly embodied the SLIP [45, Fig. 4a]. The platform used a prismatic piston leg with an air chamber providing elastic rebound. This pneumatic actuation was combined with hydraulic actuation to supply energy in stance and to place the leg in flight. The hopping robot was the first machine to demonstrate running behaviors in the sagittal plane. Subsequent generalization of this monopedal design led to bipedal and quadrupedal robots running in three dimensions [45]. The gait stability and robustness of these running machines were not well understood, triggering a chain of theoretical research on legged dynamics and control that used and further shaped the SLIP model.

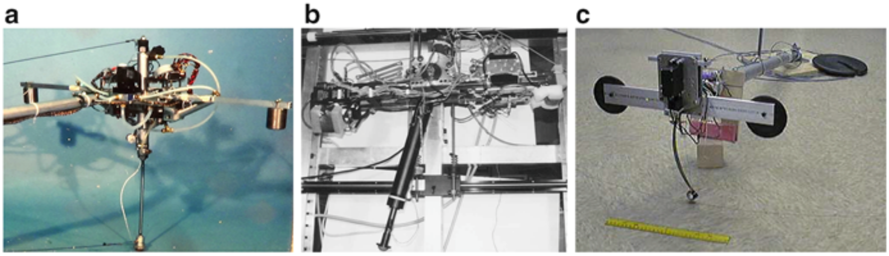

Fig. 4 Early platforms based on the SLIP model. (**a**) Raibert's monopod (Photo courtesy of B. Brown) (**b**) The ARL monopod (Photo from [1]). (**c**) The Bow-Leg monopod (Photo courtesy of G. Zeglin)

Following the success of Raibert's running robots, the ARL family of monopod robots investigated more effective mechanisms for prismatic leg actuation to regulate energy and for angular control of the leg during both flight and stance [20, Fig. 4b]. These platforms were capable of faster and more efficient running with their passive dynamic mechanisms incorporating series elastic actuation both in the radial and angular degrees of freedom [2].

The Bow-Leg platform (Fig. 4c) is an example of a Raibert-style hopper that more directly approximated the energy efficiency of the SLIP model, which does neither inject nor dissipate energy. Even though such an energetically conservative behavior is impossible to reproduce on a physical platform, the Bow-Leg platform achieved high energy efficiency by using a very lightweight leg design to minimize collision losses and a novel radial actuation mechanism that pre-compressed the leg spring during flight for discrete energy injection [69].

More recently, the emphasis for legged platforms that directly embed the SLIP model has shifted to designs that incorporate leg stiffness modulation. Animals change leg stiffness, for instance, when they run at different speeds. This observation and control theoretical results on the SLIP model have motivated robot platforms that instantiate the model with leg designs that can actively change stiffness for energy regulation and gait control. One example is the Veronica biped (Fig. 5a). Its leg stiffness regulation is based on the MACCEPA design, which uses pretension of a single spring coupled to the knee joint [64]. However, the mechanical complexity of implementing a variable leg stiffness revived the interest in platforms that can dynamically adjust the rest length of the leg spring rather than its mechanical stiffness. The ATRIAS robot (Fig. 5b) is a recent example of such robots, which uses four-bar mechanism legs with differential drive actuators concentrated at the hips. This very lightweight construction combined with series leaf springs coupling the actuators to the leg joints enables the use of force control techniques for mimicking SLIP dynamics with variable leg stiffness [21].

Other walking and running platforms exist that use compliant leg designs; however, not all of these robots have a close correspondence to the SLIP model, particularly when they use segmented morphologies that couple radial and angular

Fig. 5 Biped platforms with leg stiffness control. (**a**) The Veronica biped (Photo courtesy of D. Lefeber). (**b**) The ATRIAS biped (Photo courtesy of J. Hurst)

degrees of freedom. Examples of such robots include the KenKen leg [28], the PDR400 passive dynamic running robot [41], the Phides robot [29], and the FastRunner platform [14].

The robots summarized above exemplify the use of the SLIP model as a basis for the design of legged platforms. Animals and humans, however, show CoM dynamics similar to the SLIP model without matching its morphology (compare Sect. 1), suggesting that such a match is not necessary for the utility of springlike behavior in running gaits. This observation led to the design and construction of platforms with additional degrees of freedom, connected to the SLIP model through the idea of *embedding* its dynamics within a more complex morphology. Among earlier examples subscribing to this idea are the RHex hexapod [50, Fig. 6a] as well as the Sprawl family of hexapods [13, Fig. 6b], for which intuitive controllers optimized for efficiency led to CoM dynamics that match those of the SLIP model. More analytical approaches to SLIP embedding were later explored on the MABEL platform [62], as well as on climbing robots such as the DynaClimber [33] and ParkourBot [15]. The design of multi-legged platforms whose passive dynamics facilitate this embedding remains an active research area in robotics.

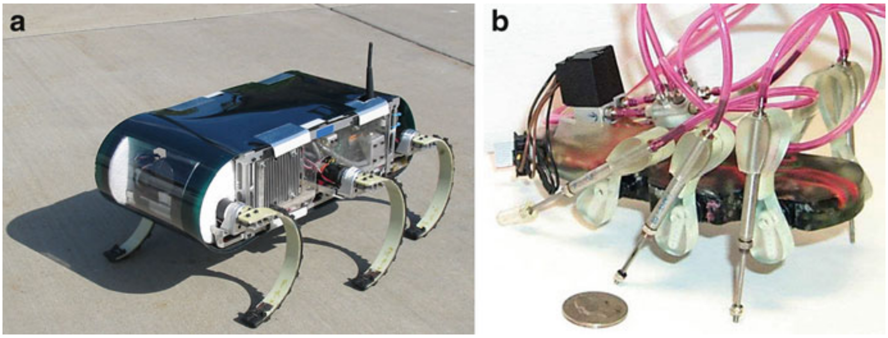

Fig. 6 Platforms embedding the SLIP model. (**a**) The RHex hexapod. (**b**) The Sprawl hexapod (Photo from [30])

Overall, the SLIP model and its variants inspired many successful robots capable of dynamic running behaviors. The next sections will describe the SLIP model in more mathematical detail, discussing methods and results obtained by studying gait dynamics and control with the SLIP model. Some of the legged platforms described here will be revisited during this discussion.

3 Planar SLIP Dynamics and Control Methods

3.1 Model Formulation

Running is a periodic behavior with recurring flight and stance phases. The planar SLIP model describes the corresponding CoM dynamics in the sagittal plane with a point mass m that moves on a ballistic trajectory in flight and rebounds on a massless spring in stance (Fig. 1a). As a result, the SLIP model forms a hybrid dynamical system with different sets of equations governing the motion in flight,

$$\begin{bmatrix} m\ddot{x} \\ m\ddot{y} \end{bmatrix} = \begin{bmatrix} 0 \\ -mg \end{bmatrix}, \tag{1}$$

and stance,

$$\begin{bmatrix} m\ddot{r} \\ \frac{d}{dt}(mr^2\dot{\theta}) \end{bmatrix} = \begin{bmatrix} mr\dot{\theta}^2 - mg\sin\theta - b\dot{r} - \frac{d}{dr}U(r) \\ mgr\cos\theta \end{bmatrix}. \tag{2}$$

In these equations, the coordinates x and y are the horizontal and vertical positions of the point mass in flight, and r and θ are the polar coordinates of the mass originating at the foot point in stance (Fig. 1a). The stance dynamics are more complicated as the spring leg produces a radial force acting on the point mass. This force is described in (2) by the general spring potential $U(r)$ (with $U(r) =$

$\frac{1}{2}k(r_0 - r)^2$ for a linear spring with stiffness k and rest length r_0) and sometimes by an additional viscous damping (coefficient b).

3.2 Return Map Analysis of Model Dynamics

The presence and stability of periodic locomotion in the SLIP model can be analyzed through *return maps*. Return or Poincaré maps result from studying how the trajectory of a periodic dynamical system evolves on a section of the state space which characterizes a repeating event [22]. Figure 7 illustrates this analysis method with the example of vertical hopping in the SLIP model ($\theta = \frac{\pi}{2}$) with damping in stance and a pre-compressed spring at landing. For vertical hopping, the state vector consists of the vertical position and velocity of the point mass, $\mathbf{z} = [y\ \dot{y}]^T$, shown in the left panel of Fig. 7. The red horizontal line marks a section of the state space which corresponds to the transition of the point mass from positive to negative velocities in the flight phase. This Poincaré section defines the *apex event*, at which the mass reaches the highest point in flight ($\dot{y} = 0$). The black and blue traces show three example trajectories $\mathbf{z}(t)$ of the model evolution between two consecutive apex events, with the blue trajectory indicating a limit cycle for which the system state at the two apex events is identical.

The right panel in Fig. 7 shows the actual return map (black line). It was generated numerically by plotting the relationship between initial apex height $y[i]$ and the next apex height $y[i+1]$ following the point mass trajectories for a range of initial heights. Because $\dot{y} = 0$ on the Poincaré section, the map is sufficient to characterize the entire system state at the apex event. In particular, the limit cycle observed in Fig. 7 appears as a fixed point intersecting the diagonal $y[i+1] = y[i]$ (blue dashed line). The fixed point confirms the presence of periodic vertical

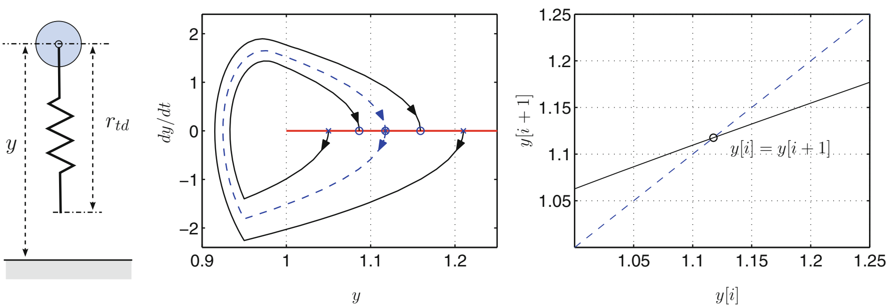

Fig. 7 Return map analysis. *Left*: Vertical SLIP model with pre-compressed leg spring. *Middle*: Evolution of the system state (phase portrait) of vertical hopping with a dissipative SLIP model ($b = 10$ Ns/m, $k = 1000$ N/m) that lands with a pre-compressed spring for energy input ($r_{td} = 0.95$ m, $r_0 = 1$ m). The *dashed blue* trajectory shows the limit cycle, and the *horizontal red line* shows the Poincaré section. *Right*: The return map (*solid black*) and its intersection with the identity map (*dashed blue*) corresponding to the limit cycle

hopping in the SLIP model. Whether this behavior is stable depends on the slope of the return map in the neighborhood of the fixed point.

In more formal language, for a given Poincaré section $\mathcal{P} \subset \mathcal{Z}$ in the state space $\mathcal{Z}$, the return map $\mathbf{R} : \mathcal{P} \rightarrow \mathcal{P}$ of an initial point $\mathbf{z}_i \in \mathcal{P}$ is defined as the first return $\mathbf{z}_{i+1}$ to the Poincaré section of the system trajectory $\mathbf{z}(t)$ evolving from $\mathbf{z}(0) = \mathbf{z}_i$:

$$\mathbf{z}_{i+1} = \mathbf{R}(\mathbf{z}_i). \tag{3}$$

The map defines a discrete dynamical system whose fixed points $\mathbf{z}^* = \mathbf{R}(\mathbf{z}^*)$ correspond to periodic trajectories of the underlying, continuous dynamical system. In addition, the stability of a fixed point can be determined by analyzing the Jacobian $D_{\mathbf{z}}\mathbf{R}|_* = \frac{\partial \mathbf{R}}{\partial \mathbf{z}}\big|_{\mathbf{z}^*}$. If all eigenvalues λ_k of the Jacobian lie within the unit circle, $\forall \lambda_k : |\lambda_k| < 1$, the fixed point, and thus the underlying periodic trajectory, is locally asymptotic stable. The reduction to fixed point analysis of the discrete return map greatly simplifies the identification and characterization of periodic locomotion in the SLIP model.

In general, the shape of the return map depends on the model parameters $\mathbf{p}$. For the later discussion of control strategies, it will be useful to consider some of these parameters as control inputs $\mathbf{u}$ whose value can change. Thus, the return map and its Jacobian at a fixed point generalize to the form

$$\mathbf{z}_{i+1} = \mathbf{R}(\mathbf{z}_i, \mathbf{u}_i, \mathbf{p}) \tag{4}$$

$$D_{(\mathbf{z},\mathbf{u})}\mathbf{R}\big|_* = \begin{bmatrix} \frac{\partial \mathbf{R}}{\partial \mathbf{z}} & \frac{\partial \mathbf{R}}{\partial \mathbf{u}} \end{bmatrix}_{(\mathbf{z}^*,\mathbf{u}^*)}. \tag{5}$$

Several points simplify the return map analysis for the SLIP model. First, dimensional analysis of the model's equations of motion, (1) and (2), shows that the parameters $\mathbf{p}$ can be combined into fewer independent groups, which reduces the parameter search space in the analysis considerably. For instance, for the SLIP model with a linear spring and no damping, only the dimensionless energy of the system, $\tilde{E}_{\text{sys}} = \frac{E_{\text{sys}}}{mgr_0}$; the dimensionless stiffness, $\tilde{k} = \frac{kr_0}{mg}$; and the landing leg angle α_0 need to be varied to describe all possible parameter dependencies of the return map [8, 17]. Second, the equations of motion are symmetric with respect to horizontal translations (and rotations in the 3-D version of the model). As a result, the *absolute* horizontal position is not important for understanding the presence and stability of periodic locomotion and can often be eliminated from the state vector $\mathbf{z}_i$. Finally, the choice of the Poincaré section can improve the intuition about the model behavior and control strategies. Common choices for the Poincaré section are the apex in flight, the touchdown or liftoff events, the midstance event ($\theta = \frac{\pi}{2}$), and the event of maximum leg compression.

Which of the model parameters are considered as control inputs $\mathbf{u}$ varies with the research question addressed using the SLIP model. The placement of the leg in the flight phase is a common task in locomotion, leading to the *leg angle of attack* at touchdown, θ_{td}, being a control input across all variations of the model.

Although this input is sufficient to modulate behavior for the conservative SLIP model ($b = 0$, constant leg stiffness, spring length at touchdown and liftoff equal to r_0), more general control strategies of running consider changes in the energy of the system. The investigated methods for energy changes in the model range from the modulation of the leg stiffness k or rest length r_0 during stance assuming a series elastic actuator along the leg axis, to the modulation of the spring length at touchdown or liftoff (compare the hopping example and Fig. 7), to the assumption of a hip torque actuator. These different modes of changing energy mirror the different designs of the legged platforms for which the SLIP model is used as a gait template in research (compare Sect. 2).

3.3 Approximate Solutions to SLIP Dynamics

The return maps can be computed by simulation of the SLIP model and then stored as lookup tables. Although this method is sufficient to analyze the model stability and derive control strategies numerically, it is difficult to establish causal relationships and draw general conclusions. As a result, there has been considerable interest in analytical versions of the return maps. However, the SLIP dynamics during stance are related to the restricted three-body problem, which does not admit a closed-form solution. In consequence, several methods have been explored to find approximate solutions that are sufficiently accurate for making predictions, while being simple enough to remain practical.

An early example of an analytic approximation was presented by [31], who approximated the Raibert hopper as an actuated ball to study the stability of vertical bouncing. They used the corresponding analytic solutions to prove global asymptotic stability for vertical hopping under particular energy pumping strategies. But these approximate solutions did not generalize well to the SLIP model, as its planar stance dynamics (2) mix ballistic motion due to gravity with a central force system generated by the spring.

One approach to overcoming this problem is to ignore gravity initially and then gradually reintegrate its effect on the dynamics. Pursuing this approach, Schwind and Koditschek [55] combined the mean value theorem with Picard iterations to develop the first approximate solutions for the lossless SLIP model. These approximations were applied by Schmitt and Holmes [53] to analyze the dynamics and stability of insect locomotion in the horizontal plane, revealing qualitative correspondence between the predicted and observed stability behavior of insect runners. The approximate solutions were also used in [19] to analytically explore the self-stable running observed for the SLIP model in the sagittal plane in a numerical simulation study by [59]. Section 3.5 will cover further details on these studies when discussing control strategies for the SLIP model.

The accuracy of the iterative solutions grows with the number of iterations used to reintegrate gravity. So does, however, the complexity of the solutions, which makes it difficult to obtain accurate predictions with low-order approximations. A second approach to approximate SLIP dynamics is to align the gravity vector with the leg axis ($\cos\theta = 0$ and $\sin\theta = 1$ in (2)), which renders the dynamics a central force system without having to neglect gravity. Geyer et al. [17] used this approach to develop an analytical solution for small angular deviations from the vertical axis and for small spring compressions. The solution was less complex and produced sufficiently accurate predictions of the self-stable SLIP behavior [59]. It was furthered and improved by [51] and [5] who incorporated viscous damping in the leg, corrected for the effect of gravity in asymmetric stance phases, and accounted for hip torque actuation. The corresponding approximate solutions have been applied for adaptive control and state estimation in running. More recently, [68] relaxed the assumption that gravity is aligned with the leg axis (by assuming $\cos\theta \approx \theta$ and $\sin\theta = 1$ in (2)) and used perturbation methods to identify an approximation which outperforms previous ones for the lossless SLIP model.

A third approach was introduced by [43], who assume an ideal actuator in series with the leg spring and implement partial feedback linearization to cancel the nonlinearities in (2). The resulting dynamics lead to approximate solutions that provide a basis for gait controllers with an actuated spring leg.

3.4 Intuitive Control Strategies

Control strategies of the planar SLIP model have evolved over time from intuitive to optimal control methods. The early control strategies go back to the 1980s. They arose from the work on legged machines that roboticists were interested in. Raibert and colleagues [45] devised an intuitive controller for their planar hopping machine (Fig. 4a), concentrating on the attitude of the center body, hopping height, and forward speed (Fig. 8). A proportional-derivative feedback on the global body angle

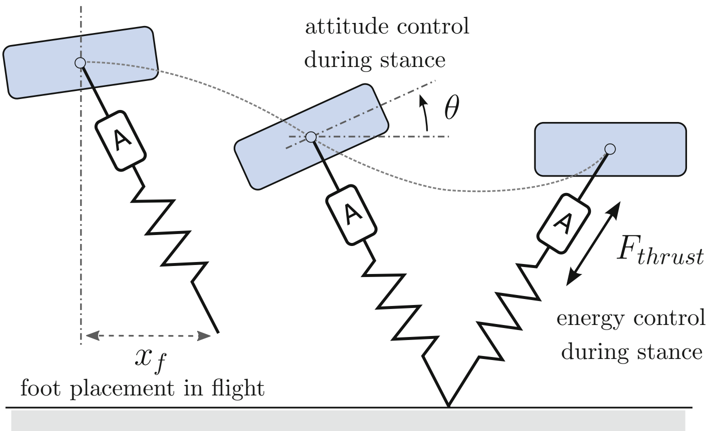

Fig. 8 Raibert's intuitive, decoupled control mechanisms: Forward speed through foot placement during flight, body attitude, and thrust control using a series actuator during stance

regulated the attitude of the center body during stance. The control of the hopping height relied on thrusting the hydraulic piston of the hopper's leg, which injected energy at maximum leg compression by shifting the rest length of the air spring that was connected in series with the piston. In effect, the duration of the thrust regulated hopping height. Finally, forward speed was regulated by foot placement in the flight phase, using a control law:

$$x_f = x_0 + c_v(\dot{x} - \dot{x}_{\mathrm{des}}), \tag{6}$$

where x_f is the horizontal leg placement target relative to the CoM, $x_0 = \dot{\bar{x}}T_s/2$ is a neutral leg placement computed from the average speed ($\dot{\bar{x}}$) and duration (T_s) of the previous stance phase, and the last term is a proportional feedback on forward speed. The neutral placement arose from the intuition that legged hopping and running are symmetric gaits and the symmetric leg placement approximately equals half the distance that the CoM advances in stance. While body attitude has no equivalent in the point mass SLIP, the thrust and forward speed controls of the Raibert hopper can be interpreted in this model. They provide intuitive examples for the control of system energy by changing the spring rest length in stance and of gait stability by leg placement in flight.

McGeer [36] combined intuition with more formal analysis of the return map of his running model to study its control (Fig. 3b). The initial version of his model had only passive spring actuation of the legs and hip. The resulting hip oscillation created a passive swing-leg placement control. The return map of this model at liftoff (denoted with a superscript)

$$\mathbf{z}_{i+1}^{lo} = \mathbf{R}(\mathbf{z}_i^{lo}, \mathbf{p}), \tag{7}$$

had five elements in the state vector $\mathbf{z}$. Parameter sets $\mathbf{p}$ can be found in simulation for which the model indicates steady running with $\mathbf{z}_{i+1}^{lo} = \mathbf{z}_i^{lo} = \mathbf{z}_*^{lo}$. Some of these solutions have eigenvalues λ_j of the Jacobian $D_{\mathbf{z}}\mathbf{R}|_*$ that lie within the unit circle ($|\lambda_j| < 1$), which showed that the running model can be passively stable. Although McGeer never built a passive dynamic running robot, several such machines have been demonstrated over time [41, 46].

In addition, McGeer used the return map to study active control during stance of his running model. He reasoned about several options from torquing the hip to thrusting the leg to increasing its spring rest length in proportion to stance progression. In particular, the latter control strategy produces a leg force $F = k(r_0^\dagger - r)$, where the rest length $r_0^\dagger = r_0 + c_\alpha(\theta - \pi/2)$ is modulated by the leg angle swept in stance. Treating the gain parameter c_α as a thrust control input, he then proceeded to compute the sensitivity $D_{\mathbf{u}}\mathbf{R} = \partial\mathbf{R}/\partial c_\alpha$ of the return map to this input, resulting in the linearized error dynamics

$$\mathbf{z}_{i+1}^{lo} - \mathbf{z}_*^{lo} = \mathbf{A}\,(\mathbf{z}_i^{lo} - \mathbf{z}_*^{lo}) + \mathbf{B}\,(c_\alpha - c_{\alpha *}) \tag{8}$$

of the biped model about a steady-state solution (indicated by the asterisk) with the dynamics matrix $\mathbf{A} = D_{\mathbf{z}}\mathbf{R}|_*$ and the control vector $\mathbf{B} = D_{\mathbf{u}}\mathbf{R}|_*$. Using LQR, he derived an optimal state feedback control $c_\alpha(\mathbf{z}^{lo})$ that simultaneously regulated all five states of the biped model, actively stabilizing running within a small neighborhood of the steady-state solution.

Although the early control strategies depended on intuition, they established the fundamental concepts and methods that are being used to study the control of spring-legged running today.

3.5 SLIP Control Derived from Return Maps

Control strategies specific to the SLIP model evolved from the formal analysis of the Raibert hopper with successively simpler gait models. M'Closkey and Burdick [37] modeled the hopper with a SLIP that has an "air spring" force law $F \sim 1/r$. They considered Raibert's control of leg thrust after midstance and of foot placement in flight. Analyzing an approximate return map between consecutive midstances of this model, they found that the control could lead to period doubling and chaotic behavior. Schwind and Koditschek [54] further reduced this model by ignoring thrust and focusing solely on leg placement. They introduced the apex return map $\mathbf{z}^a_{i+1} = R(\mathbf{z}^a_i, \mathbf{p})$ of the SLIP with the Poincaré section coordinates $\mathbf{z}^a := [y^a\ \dot{x}^a]^T$ and numerically solved for leg placement angles θ_{td} which will generate symmetric stance phases with equal touchdown and takeoff angles of the leg, $\theta_{lo}(\mathbf{z}^a_i, \theta_{td}) = \pi - \theta_{td}$, starting from an initial state $\mathbf{z}^a_i$ (Fig. 1a). They used these solutions to show that a corresponding leg placement control which assumes

$$\mathbf{z}^a = \begin{bmatrix} y^a \\ \dot{x}_* + k(\dot{x}_* - \dot{x}^a) \end{bmatrix} \tag{9}$$

leads to better regulation and a larger basin of attraction than the original Raibert leg placement.

Inspiration from biology further clarified the model and control understanding. In cockroach running, perturbations diminish without intervention by the neural system, suggesting that no active control of leg placement is needed, and passive dynamics are sufficient to stabilize gait. Inspired by this observation, Schmitt and Holmes [53] used the simple SLIP to study horizontal plane stability of locomotion in these animals. With an interest in understanding passive stabilization, they assumed a constant angle of the swing leg before landing and found self-stabilizing behavior. Shortly after, Seyfarth and colleagues observed a similar self-stabilization of the SLIP in the sagittal plane when modeling human running [59].

Figure 9 shows an example of self-stabilization using the apex return map of the simple SLIP for human running. In this model, the swing leg is set to a constant angle $\theta_{td} = \alpha_0$ with respect to the world frame once the apex event is passed (Fig. 9a). For studying gait stability, the corresponding apex return map,

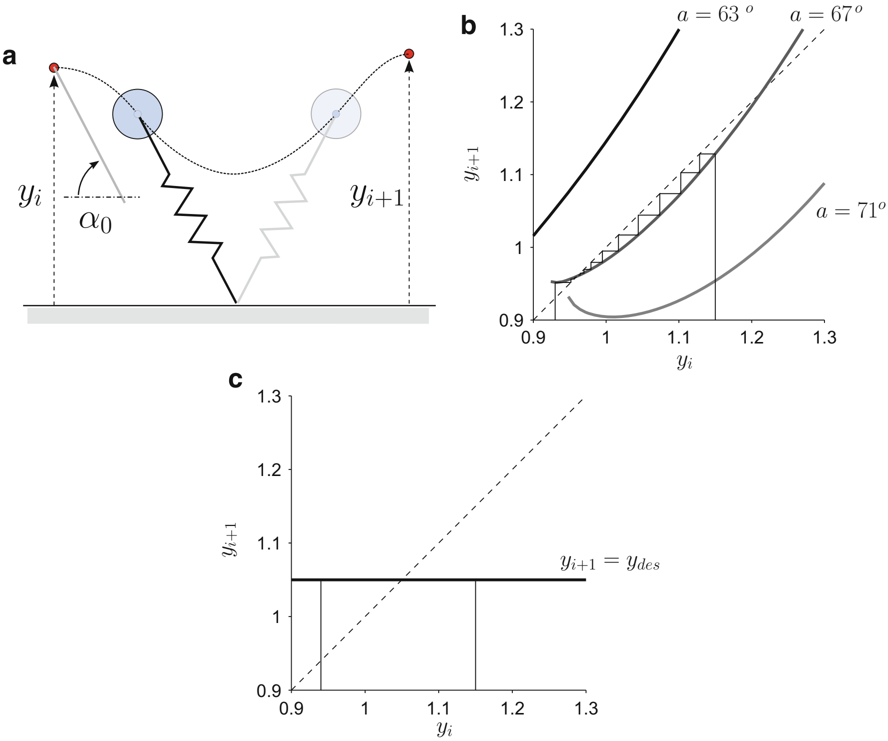

Fig. 9 Gait stability of SLIP running. (**a**) SLIP model assuming constant swing-leg angle once apex is passed. (**b**) Apex return map for three different swing-leg angles. Return map for $\alpha =$ 68 deg has stable periodic solution. *Arrow traces* indicate apex states of subsequent steps starting from two different initial conditions (i and ii). Model parameters fit human running [59]. (**c**) Super-stable return map indicating deadbeat control of target state y_{des}

$\mathbf{z}^a_{i+1} = R(\mathbf{z}^a_i, \mathbf{p})$, reduces to mapping a single state, the apex height with $\mathbf{z}^a := y^a$. The reduction is possible as the landing condition $y_{td} = r_0 \sin \alpha_0$ defined by α_0 does not depend on forward progression [59]. Figure 9b sketches three such return maps for three different angles α_0. While not every return map indicates stable periodic solutions, swing-leg angles can be found that stabilize SLIP running (for instance, $\alpha = 68°$) without active regulation of the swing leg angle by forward speed.

More recent parameter studies have further mapped out the stability properties of intuitive SLIP control strategies with the same method. Examples include the proportional regulation of the leg angle, length or stiffness prior to touchdown, and the regulation of the leg angle based on a constant aperture with the stance leg [4]. These studies demonstrate that different control strategies lead to stable locomotion in the SLIP, revealing control alternatives for animals and robots. However, alternatives also complicate the formulation of a unified theory of SLIP control.

The transition to optimal control strategies provides a more formal approach to SLIP control. If a target state $\mathbf{z}^a_{\text{des}}$ is introduced and some model parameters are considered as inputs $\mathbf{u}$ (compare Sect. 3.2), SLIP control can be interpreted as searching for values

$$\mathbf{u}_i = \underset{\mathbf{u}}{\operatorname{argmin}}\ d\left[\mathbf{z}^a_{\text{des}}, \mathbf{R}(\mathbf{z}^a_i, \mathbf{u}, \mathbf{p})\right] \tag{10}$$

of the input $\mathbf{u}$ that force the SLIP from the current state $\mathbf{z}^a_i$ into the target state over the course of one step. In this optimization problem, $d[.,.]$ is an appropriate measure of distance between apex states (for instance, the Euclidean norm). A parameter policy $\mathbf{u}_i(\mathbf{z}^a_i)$ that brings the distance to zero for all initial states describes deadbeat control (Fig. 9c). This approach has been used by several researchers to study leg placement in flight. It led to generalized swing-leg policies that make the SLIP reject unknown ground disturbances [60] or limit leg force production [10]. These results helped to interpret the leg retraction observed in animals right before landing in the light of gait stability or injury avoidance and to understand that the original Raibert speed control of (6) locally approximates the swing-leg policies for ground disturbance rejection [67].

To study the control of system energy, the simple and conservative SLIP model has been extended. Canonical extensions include tuning the spring stiffness or spring rest length with a series actuator and torquing the hip (Fig. 10). With these extensions, early studies relied on parameter sweeps of intuitive control strategies, showing stabilized running of the model with clock-based leg angle control throughout the gait cycle [58] and spring rest length control throughout stance [52]. More recently, optimal control problems similar to (10) have been explored with a focus on series leg actuation in stance, deriving the necessary actuation for deadbeat control of hopping height and forward velocity at apex [48, 56]. In both cases, approximate solutions of the extended SLIP have been used, for instance, to perform online model predictive control in multistep problems. In general, these control solutions are more energy efficient than the original idea of pumping energy after midstance used in the Raibert controller (compare Sect. 3.4).

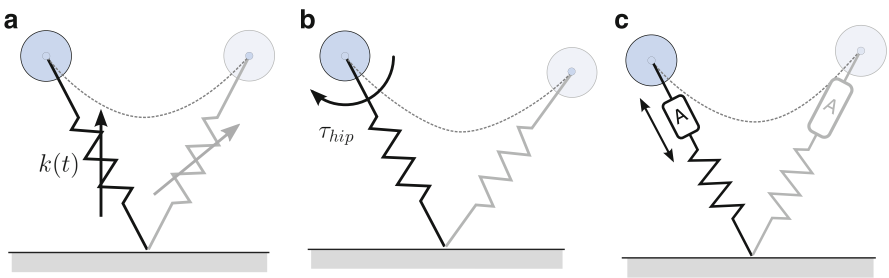

Fig. 10 Mechanisms for energy regulation for the SLIP model. (**a**) Time-varying tunable spring stiffness during stance. (**b**) Torquing the hip. The point mass is assumed to have infinite rotational inertia. (**c**) Shifting the spring rest length with a series actuator

4 Generalizations

The analysis methods and control strategies discussed in Sect. 3 focus on a single stride with the planar SLIP model. These methods and strategies have been generalized to multistep planning, locomotion in 3-D environments, walking and gait transitions, and embedding in humanoids and other legged robots.

4.1 Multistep Planning

The first algorithms that explicitly consider multiple steps in locomotion on spring legs go back to the 1990s. Based on the low level stride controllers adopted by Raibert's runners, Hodgins and Raibert [25] introduced three alternatives for adjusting step length to indirectly perform footstep planning for locomotion on rough terrain. They found that regulating forward running speed for controlling step length, while using the remaining degrees of freedom to ensure dynamic balance, was the most successful among available alternatives. A related study by [24] investigated how multiple steps can be used to prepare for a backflip with Raibert's bipeds, followed by additional steps to recover balance and achieve steady state.

A more systematic approach to multistep planning was presented by [69] for the Bow-Leg hopper. This study proposed a search strategy across a discretized space of possible leg placement angles, which were evaluated by a cost function that captures different aspects of the gait such as the safety of the footholds, energetic costs associated with the step, the friction cone for the toe, as well as distance to the goal. The planner was demonstrated both in simulation and on the planar Bow-Leg robot. Recent related work on footstep planning includes the use of model predictive control (MPC) to plan for a fixed number of upcoming footholds, which are then realized through a single-step controller to reduce the accumulation of the foot placement error [48].

An alternative to such model-based, feed-forward strategies was explored in [7], where a reactive framework was introduced for multistep control that is robust to model and sensory uncertainties. The framework relies on dynamically accurate approximation of a single stride to construct a cover for the apex Poincaré section, associating every state with a particular control policy. The resulting reactive controller can generate complex goal-oriented sequences of footsteps while being fully reactive and, hence, robust to model and sensor uncertainties.

4.2 Running in 3-D Environments

Although steady walking and running are mainly sagittal plane behaviors, legged animals and robots maneuver in a three-dimensional world. Several studies have generalized the SLIP model to better understand the effect of the extra dimension on the dynamics and control of locomotion.

The Raibert hoppers were the first robots to realize 3-D locomotion on springy legs [45]. The hoppers duplicated the pitch and swing-leg placement controls of the sagittal plane motion (compare Sect. 3.4) to control roll and leg placement in the frontal plane. Based on the assumption that the sagittal and frontal plane dynamics are only weakly coupled, this intuitive control generalization realized 3-D hopping with a stabilized attitude of the center body and with controlled changes in the heading direction. It did not account for changes in the facing direction, although Raibert and colleagues reasoned about an explicit yaw control of the center body through alternating leg placement. Their idea used the fact that foot placement away from the hopping robot causes pitch, roll, and yaw disturbances. The pitch and roll disturbances can be canceled with opposing leg placements in two steps, leaving a net yaw correction [45].

The first detailed analysis of the 3-D SLIP model was done by Carver and colleagues. They investigated deadbeat leg placement policies and found that, in general, multiple steps are required to recover from gait perturbations [11]. More recent works in this area focus on feedforward leg placement strategies, finding unstable running when the swing leg is placed with respect to the world frame [57] and stabilizing behavior when it is placed with respect to the direction of motion at apex [42]. In addition, feedforward placement policies have been identified that generalize the swing-leg policies for large ground disturbance rejection (Sect. 3.5) to include deadbeat turning [67].

4.3 Walking and Gait Transitions

The SLIP model can describe not only running but also walking. Already in the 1980s, a spring leg model was used to explore the biomechanics of walking before the SLIP became the common tool for studying running. In a biomechanical study on horse walking, van Gurp et al. [63] modeled the hind limbs of horses with a spring leg loaded by a time-varying point mass $M(t)$ (Fig. 11a). The variable mass accounted for the effect of load sharing induced by the other hind limb during the double-support phase, and the model mimicked the ground reaction forces observed in walking horses. These forces are similar to the ground reaction forces found in human walking.

Despite the similarity, van Gurp and colleagues' work did not gain attention in the biomechanics and robotics communities, and the rigid inverted pendulum grew into the basic template for walking mechanics (see chapter "▸ Linear Inverted Pendulum Based Gait" in this book). For instance, Hodgins [23] demonstrated gait transitions between walking and running with the bipedal version of the Raibert hopper by controlling the robot to mimic an inverted pendulum motion in walking.

Spring leg walking resurfaced as a theoretical model about 10 years ago. Geyer et al. [18] were interested in a gait template that better resembles the dynamics of walking than the rigid inverted pendulum. They extended the SLIP model with constant point mass to a bipedal version and found that the walking and running dynamics of animals and humans are just two out of many solutions to

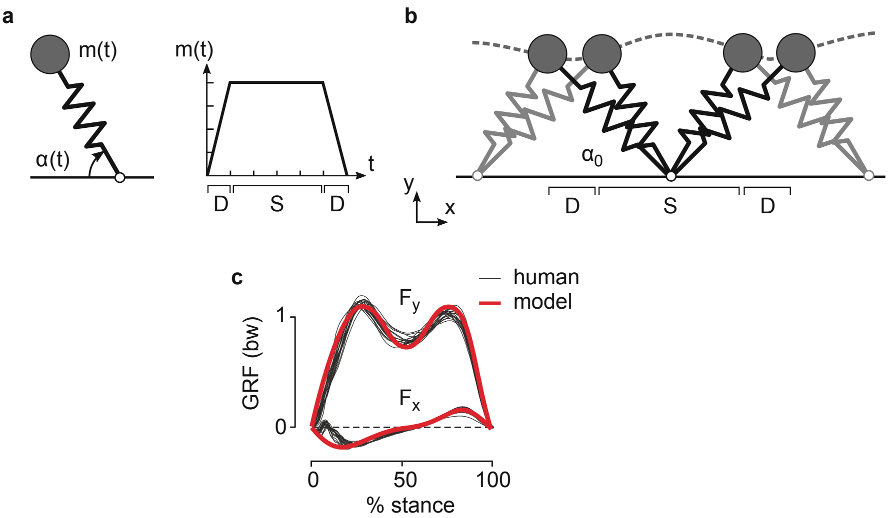

Fig. 11 Walking with the SLIP model. (**a**) Spring leg loaded by a time-varying mass m(t) to describe load sharing during double support (D) in walking. (**b**) Bipedal SLIP model assuming constant swing-leg angle once apex is passed in single support (S). (**c**) Ground reaction forces (GRFs) in walking for humans (*thin traces*) and the bipedal SLIP (*thick traces*)

legged locomotion offered by compliant leg behavior (Fig. 11b, c). A subsequent experimental comparison showed that the bipedal SLIP well describes the whole body dynamics for human walking at moderate speeds, but deviations occur at slow and fast speeds [32]. More recent work led to model extensions including roller feet and leg damping, which improved the match between the ground reaction forces observed in humans and produced by the bipedal SLIP model [e.g., 66]. Finally, the model has been extended to 3-D walking using the same control technique of a constant leg placement with respect to the current direction of motion as used for 3-D running [35].

As a combined model for walking and running, the bipedal SLIP makes it possible to study the dynamics and control of gait transitions within a unified theoretical framework. Although gait transitions in animals and humans are often associated with a change in speed or locomotion energy, Salazar and Carbajal [34] investigated if control strategies exist in this model that generate transitions without having to add or remove system energy. They showed that such transitions can be induced by properly sequencing the swing-leg angle of attack over several steps. For the run-to-walk transition, this sequence needs to pass through grounded running, a gait with walking-like double supports and running-like ground reaction forces found in animals [3] and the bipedal SLIP [47]. On the other hand, Shahbazi and colleagues [61] added leg stiffness modulation to alter the model's system energy. Using the optimal control approach outlined in (10), they identified a control policy that generates speed and gait transitions by adapting the stance leg stiffness in addition to the swing-leg angle of attack. For the transitions, the model does not need to pass through grounded running, and its motion resembles the motion of the CoM in human gait transitions.

4.4 Embedding in Humanoids and Other Legged Robots

Humanoids and other legged robots are more complex dynamical systems than the simple SLIP model represents. The SLIP and its variants are abstract gait templates that trade realism for mathematical simplicity, yielding general control strategies for legged locomotion. Different approaches have been pursued to embed these strategies in more complex legged robots. They have in common that the template behavior is mapped onto the degrees of freedom of the more complex legged robot with techniques similar to operational space control.

Simplified approaches consider the legged robot as a rigid body with massless legs and map an imagined wrench $\boldsymbol{F}_{\text{body}}^{\text{des}}$ acting on this body into the joint torques

$$\boldsymbol{\tau} = \boldsymbol{J}^T \boldsymbol{F}_{\text{body}}^{\text{des}}, \tag{11}$$

using the Jacobian $\boldsymbol{J}$. Example approaches include virtual leg control and, more generally, virtual model control. In virtual leg control, the net forces and torques generated by two or more physical legs on the center body of a robot are made equal to the wrench applied by a virtual leg (Fig. 12a). Raibert and colleagues [45] used this approach to map the control developed for their one-legged hopper onto quadrupedal machines. The control algorithms reviewed in Sect. 3.4 operated on a virtual one-legged hopper, and the resulting net wrench applied by the hopper's leg was distributed to the physical legs of the quadrupedal machine under the constraint that the axial forces of the legs on the ground in synchrony are equal. Saranli and colleagues [49] applied the same quasi-static torque mapping to specifically embed the SLIP model acting between the toe and the hip of a simulated segmented

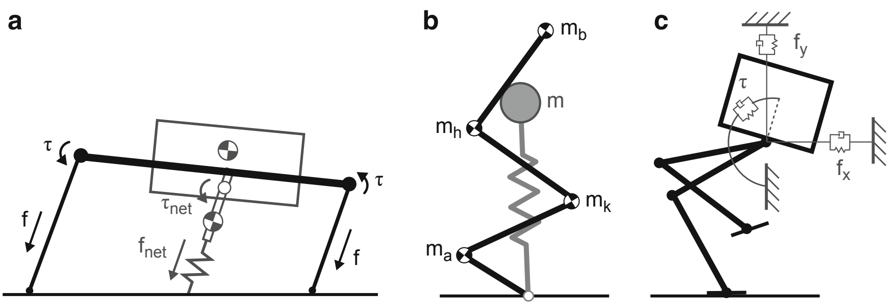

Fig. 12 Mapping simple gait models to legged robots. (**a**) Virtual leg control with physical legs producing imagined action of a virtual one-legged hopper [45]. (**b**) Explicit mapping of the SLIP into more complex leg model in simulation [49]. (**c**) Generalization to virtual model control [44]

leg (Fig. 12b). Later, the concept of quasi-static mapping has been generalized to arbitrary model systems. Using virtual spring and damper models acting on the center body, Pratt and colleagues [44] devised an intuitive walking control for their bipedal robot "spring turkey" (Fig. 12c).

Recent approaches to embedding the SLIP take the full rigid body dynamics of legged robots into account. Sreenath and colleagues [62] applied control techniques from hybrid zero dynamics to design a feedback controller for the robot dynamics model:

$$\boldsymbol{M}\ddot{\boldsymbol{q}} + \boldsymbol{h} = \boldsymbol{S}^T\boldsymbol{\tau} + J^T\boldsymbol{F}_{\text{ext}}, \tag{12}$$

that embeds a virtual spring behavior in the stance leg. They demonstrated with this controller running at 3 m/s of the MABEL robot constrained to a boom (Fig. 5a). More often, the SLIP is embedded as the target for the translational dynamics of the CoM of the entire robot using direct operational space control methods. For instance, Hutter and colleagues [27] use the projection method to derive the joint torques

$$\boldsymbol{\tau} = J^{*T}\left[\boldsymbol{\Lambda}^*\ddot{\boldsymbol{r}}_{CoM} + \boldsymbol{\mu}^* + \boldsymbol{p}^*\right] \tag{13}$$

that impose SLIP behavior $\ddot{\boldsymbol{r}}_{CoM} = \frac{1}{m}(\boldsymbol{F}_{\text{spr}} + m\boldsymbol{g})$ of the CoM by compensating for the effects of inertia terms ($\boldsymbol{\Lambda}^*$), Coriolis and centrifugal terms ($\boldsymbol{\mu}^*$), and gravitational terms ($\boldsymbol{p}^*$) perceived in task space (indicated by asterisk). A similar approach was used in [6] to achieve planar pronking with an underactuated hexapod model, relying on passive leg compliance to match radial SLIP dynamics. The work of Wensing and Orin [65], on the other hand, provides an example for the quadratic programming method:

$$\begin{aligned} \min_{\ddot{\boldsymbol{q}},\boldsymbol{\tau},\boldsymbol{F}} \quad & \frac{1}{2}||\boldsymbol{A}\ddot{\boldsymbol{q}} + \dot{\boldsymbol{A}}\dot{\boldsymbol{q}} - \dot{\boldsymbol{\rho}}||^2 \\ s.t. \quad & \boldsymbol{M}\ddot{\boldsymbol{q}} + \boldsymbol{h} = \boldsymbol{S}^T\boldsymbol{\tau} + J^T\boldsymbol{F}_{\text{ext}} \\ & \boldsymbol{\tau} \in [\boldsymbol{\tau}_{\min}, \boldsymbol{\tau}_{\max}] \\ & \ldots, \end{aligned} \tag{14}$$

to optimally balance matching the SLIP behavior against other behavior goals (collectively described by a task Jacobian $\boldsymbol{A}$ and a desired task dynamics vector $\dot{\boldsymbol{\rho}}$) and against constraints on the dynamics of a simulated humanoid robot. In both cases, the SLIP model's deadbeat control, (10), or a local approximation of it (similar to (8)) is used as an outer loop control to obtain locomotion robustness. Although the operational space control methods can today achieve real-time control rates of several hundred hertz, actual robot implementations and evaluations of the resulting SLIP-based controllers remain pending.

5 Future Directions and Open Problems

The spring-loaded inverted pendulum has evolved from a basic gait template for studying running biomechanics into a versatile tool for designing and controlling legged robots. This evolution has advanced the analytical description of the model, produced control strategies for agile and robust locomotion on compliant legs, and led to initial robot implementations of some of these strategies. To grow the model's utility, future directions will likely focus on the generalization of the model's approximate solutions and their use in planning and state estimation of compliant robots, the hierarchical expansion of the model beyond a point mass system, and more implementation and verification of the model-predicted control strategies in legged robots including humanoids.

Analytical approximate solutions to the SLIP dynamics have so far focused on sagittal plane running. The more recent adaptation of the model to describing running and walking in 3-D environments creates demand for approximate solutions to the model dynamics in more complex environments and for more complex gaits. In addition, an increasing adoption of the model in designing control strategies for legged robots will require a better understanding of the utility of these approximate solutions for real-time planning and estimation of the robot state in locomotion.

Hierarchical model expansions which increase realism is another direction that fuels future research. The expansions comprise the generalization of the robust control strategies developed for running to SLIP-based walking. They also comprise the substitution of the point mass with a rigid center body to address the inherent coupling between leg placement and the body's pitch, roll, and yaw in compliant legged systems. Finally, it will be necessary to better understand which control strategies of the SLIP can be modularized and, thus, generalized to individual limb control of multi-legged animals and robots including quadrupeds and hexapods.

Beyond progress in theoretical work on SLIP-based gait, there is demand for more testing of the utility of these theories for the design and control of legged robots. Verifications of the developed theories should lead to more agile and robust behavior in legged robots. On the other hand, falsifications will help to pinpoint gaps in the current understanding and to direct future theoretical work. Despite the benefit of this interaction between theory and experiment, implementations and evaluations of the SLIP-based control strategies on robot platforms largely remain pending. A more rigorous and concerted research effort in this direction will likely accelerate progress on the science and technology of SLIP-based gait in legged systems.

References

1. M. Ahmadi, M. Buehler, Preliminary experiments with an actively tuned passive dynamic running robot. Exp. Robot. **V**, 312–324 (1998)
2. M. Ahmadi, M. Buehler, Controlled passive dynamic running experiments with the ARL-monopod II. IEEE Trans. Robot. **22**(5), 974–986 (2006)
3. R. Alexander, A. Jayes, Vertical movements in walking and running. J. Zool. **185**(1), 27–40 (1978)

4. E. Andrada, C. Rode, R. Blickhan, Grounded running in quails: simulations indicate benefits of observed fixed aperture angle between legs before touch-down. J. Theor. Biol. **335**, 97–107 (2013)
5. M.M. Ankarali, U. Saranli, Stride-to-stride energy regulation for robust self-stability of a torque-actuated dissipative spring-mass hopper. Chaos: Interdisciplinary J. Nonlinear Sci. **20**(3), 033121 (2010)
6. M.M. Ankarali, U. Saranli, Control of underactuated planar pronking through an embedded spring-mass hopper template. Auton. Rob. **30**(2), 217–231 (2011). https://doi.org/10.1007/s10514-010-9216-x
7. O. Arslan, U. Saranli, Reactive planning and control of planar spring-mass running on rough terrain. IEEE Trans. Robot. **28**(3), 567–579 (2012)
8. R. Blickhan, The spring-mass model for running and hopping. J. Biomech. **22**, 1217–1227 (1989)
9. R. Blickhan, R.J. Full, Similarity in multilegged locomotion: bouncing like a monopode. J. Comp. Physiol. A **173**(5), 509–517 (1993)
10. Y. Blum, H.R. Vejdani, A.V. Birn-Jeffery, C.M. Hubicki, J.W. Hurst, M.A. Daley, Swing-leg trajectory of running guinea fowl suggests task-level priority of force regulation rather than disturbance rejection. PLoS One **9** (2014)
11. G.S. Carver, N.J. Cowan, J.M. Guckenheimer, Lateral stability of the spring-mass hopper suggests a two-step control strategy for running. Chaos **19**(2), 26106–26114 (2009)
12. G.A. Cavagna, F.P. Saibene, R. Margaria, Mechanical work in running. J. Appl. Physiol. **19**(2), 249–256 (1964)
13. J.G. Cham, S.A. Bailey, J.E. Clark, R.J. Full, M.R. Cutkosky, Fast and robust: hexapedal robots via shape deposition manufacturing. Int. J. Robot. Res. **21**(10), 869–882 (2002)
14. S. Cotton, I.C. Olaru, M. Bellman, T. van der Ven, J. Godowski, J. Pratt, FastRunner: a fast, efficient and robust bipedal robot. Concept and planar simulation, in *Proceedings of IEEE International Conference on Robotics and Automation*, 2012, pp. 2358–2364
15. A. Degani, S. Feng, H.B. Brown, K.M. Lynch, H. Choset, M.T. Mason, The ParkourBot – a dynamic BowLeg climbing robot, in *Proceedings of IEEE International Conference on Robotics and Automation*, 2011, pp. 795–801
16. C.T. Farley, D.P. Ferris, Biomecahnics of walking and running: center of mass movements to muscle action. Exerc. Sport Sci. Rev. **26**, 253–283 (1998)
17. H. Geyer, A. Seyfarth, R. Blickhan, Spring-mass running: simple approximate solution and application to gait stability. J. Theor. Biol. **232**(3), 315–328 (2005)
18. H. Geyer, A. Seyfarth, R. Blickhan, Compliant leg behaviour explains the basic dynamics of walking and running. Proc. R. Soc. Lond. B **273**, 2861–2867 (2006)
19. R.M. Ghigliazza, R. Altendorfer, P. Holmes, D. Koditschek, A simply stabilized running model. SIAM J. Appl. Dyn. Syst. **2**, 187–218 (2003)
20. P. Gregorio, M. Ahmadi, M. Buehler, Design, control, and energetics of an electrically actuated legged robot. Trans. Syst. Man Cybern. B Cybern. **27**(4), 626–634 (1997)
21. J.A. Grimes, J.W. Hurst, The design of ATRIAS 1.0 a unique monopod, hopping robot, in *Proceedings of the International Conference on Climbing and Walking Robots*, 2012, pp. 467–474
22. J. Guckenheimer, P. Holmes, *Nonlinear Oscillations, Dynamical Systems, and Bifurcations of Vector Fields* (Springer, New York, 2002)
23. J.K. Hodgins, Biped gait transitions, in *Proceedings of IEEE International Conference on Robotics and Automation*, 1991, pp. 2092–2097
24. J. Hodgins, M.H. Raibert, Biped gymnastics. Int. J. Robot. Res. **9**(2), 115–132 (1990)
25. J.K. Hodgins, M.N. Raibert, Adjusting step length for rough terrain locomotion. IEEE Trans. Robot. Automat. **7**(3), 289–298 (1991)
26. J.W. Hurst, The electric cable differential leg: a novel design approach for walking and running. Int. J. Hum. Robot. **08**(02), 301–321 (2011)

27. M. Hutter, C.D. Remy, M.A. Hopflinger, R. Siegwart, SLIP running with an articulated robotic leg, in *Proceedings of IEEE/RSJ International Conference on Intelligent Robots and Systems*, 2010, pp. 4934–4939
28. S.H. Hyon, T. Mita, Development of a biologically inspired hopping robot-"Kenken", in *Proceedings of IEEE International Conference on Robotics and Automation*, vol. 4, 2002, pp. 3984–39914
29. J.G.D. Karssen, M. Haberland, M. Wisse, S. Kim, The effects of swing-leg retraction on running performance: analysis, simulation, and experiment. Robotica **33**(10), 2137–2155 (2015)
30. S. Kim, J.E. Clark, M.R. Cutkosky, isprawl: autonomy, and the effects of power transmission, in Climbing and Walking Robots (Springer, Berlin/New York), 859–867 (2005)
31. D.E. Koditschek, M. Buehler, Analysis of a simplified hopping robot. Int. J. Robot. Res. **10**(6), 587–605 (1991)
32. S.W. Lipfert, M. Gunther, D. Renjewski, S. Grimmer, A. Seyfarth, A model-experiment comparison of system dynamics for human walking and running. J. Theor. Biol. **292**, 11–17 (2012)
33. G.A. Lynch, J.E. Clark, P.-C. Lin, D.E. Koditschek, A bioinspired dynamical vertical climbing robot. Int. J. Robot. Res. **31**(8), 974–996 (2012)
34. H.R. Martinez Salazar, J.P. Carbajal, Exploiting the passive dynamics of a compliant leg to develop gait transitions. Phys. Rev. E **83** (2011)
35. H.-M. Maus, A. Seyfarth, Walking in circles: a modelling approach. J. R. Soc. Interface **11**(99) (2014)
36. T. McGeer, Passive bipedal running. Proc. Royal Soc. B **240**, 107–134 (1990)
37. R.T. M'Closkey, J.W. Burdick, Periodic motions of a hopping robot with vertical and forward motion. Int. J. Robot Res. **12**, 197–218 (1993)
38. T.A. McMahon, G.C. Cheng, The mechanism of running: how does stiffness couple with speed? J. Biomech. **23**, 65–78 (1990)
39. T.A. McMahon, P.R. Greene, Fast running tracks. Sci. Am. **239**(6), 148–163 (1978)
40. T.A. McMahon, G. Valiant, E.C. Frederik, Groucho running. J. Appl. Physiol. **62**(6), 2326–2337 (1987)
41. D. Owaki, M. Koyama, S. Yamaguchi, S. Kubo, A. Ishiguro, A two-dimensional passive dynamic running biped with knees, in *Proceedings of IEEE International Conference on Robotics and Automation*, 2010, pp. 5237–5242
42. F. Peuker, C. Maufroy, A. Seyfarth, Leg-adjustment strategies for stable running in three dimensions. Bioinspir. Biomim. **7**(3), 036002 (2012)
43. G. Piovan, K. Byl, Enforced symmetry of the stance phase for the spring-loaded inverted pendulum, in *Proceedings of IEEE International Conference on Robotics and Automation*, 2012, pp. 1908–1914
44. J. Pratt, C.-M. Chew, A. Torres, P. Dilworth, G. Pratt, Virtual model control: an intuitive approach for bipedal locomotion. Int. J. Robot. Res. **20**(2), 129–143 (2001)
45. M.H. Raibert, *Legged Robots That Balance* (MIT press, Cambridge, 1986)
46. R. Ringrose, Self-stabilizing running, in *Proceedings of IEEE International Conference on Robotics and Automation*, vol. 1, 1997, pp. 487–493
47. J. Rummel, Y. Blum, A. Seyfarth, Robust and efficient walking with spring-like legs. Bioinspir. Biomim. **5**, 046004 (2010)
48. M. Rutschmann, B. Satzinger, M. Byl, K. Byl, Nonlinear model predictive control for rough-terrain robot hopping, in *Proceedings of IEEE/RSJ International Conference on Intelligent Robots and Systems*, 2012, pp. 1859–1864
49. U. Saranli, W.J. Schwind, D.E. Koditschek, Towards the control of a multi-jointed, monoped runner, Leuven, Belgium, in *Proceedings of IEEE International Conference on Robotics and Automation*, 1998, pp. 2676–2682
50. U. Saranli, M. Buehler, D.E. Koditschek, RHex: a simple and highly mobile robot. Int. J. Robot. Res. **20**(7), 616–631 (2001)

51. U. Saranli, O. Arslan, M.M. Ankarali, O. Morgul, Approximate analytic solutions to non-symmetric stance trajectories of the passive spring-loaded inverted pendulum with damping. Nonlinear Dyn. **62**(4), 729–742 (2010)
52. J. Schmitt, J. Clark, Modeling posture-dependent leg actuation in sagittal plane locomotion. Bioinspir. Biomim. **4**(4), 46005 (2009)
53. J. Schmitt, P. Holmes, Mechanical models for insect locomotion: dynamics and stability in the horizontal plane I. Theory. Biol. Cybern. **83**(6), 501–515 (2000)
54. W.J. Schwind, D.E. Koditschek, Control of forward velocity for a simplified planar hopping robot, in *Proceedings of IEEE International Conference on Robotics and Automation*, vol. 1, 1995, pp. 691–696
55. W.J. Schwind, D.E. Koditschek, Approximating the stance map of a 2-DOF Monoped runner. J. Nonlinear Sci. **10**, 533–568 (2000)
56. G. Secer, U. Saranli, Control of hopping through active virtual tuning of leg damping for serially actuated legged robots, in *Proceedings of IEEE International Conference on Robotics and Automation*, Hong Kong, 2014, pp. 4556–4561
57. J.E. Seipel, P. Holmes, Running in three dimensions: analysis of a point-mass sprung-leg model. Int. J. Robot. Res. **24**(8), 657–674 (2005)
58. J. Seipel, P. Holmes, A simple model for clock-actuated legged locomotion. Regul. Chaotic Dyn. **12**, 502–520 (2007)
59. A. Seyfarth, H. Geyer, M. Günther, R. Blickhan, A movement criterion for running. J. Biomech. **35**, 649–655 (2002)
60. A. Seyfarth, H. Geyer, H.M. Herr, Swing-leg retraction: a simple control model for stable running. J. Exp. Biol. **206**, 2547–2555 (2003)
61. M. Shahbazi, G.A.D. Lopes, R. Babuska, Automated transitions between walking and running in legged robots, in *Proceedings of the World Congress, International Federation of Automatic Control*, 2014, pp. 2171–2176
62. K. Sreenath, H.-W. Park, I. Poulakakis, J.W. Grizzle, Embedding active force control within the compliant hybrid zero dynamics to achieve stable, fast running on MABEL. Int. J. Robot. Res. **32**(3), 324–345 (2013)
63. M. van Gurp, H.C. Schamhardt, A. Crowe, The ground reaction force pattern from the hindlimb of the horse simulated by a spring model. Acta. Anat. **129**, 31–33 (1987)
64. B. Vanderborght, N. Tsagarakis, R. Ham, I. Thorson, D. Caldwell, MACCEPA 2.0: compliant actuator used for energy efficient hopping robot chobino1d. Auton. Rob. **31**, 55–65 (2011)
65. P.M. Wensing, D.E. Orin, High-speed humanoid running through control with a 3D-SLIP model, in *Proceedings of IEEE/RSJ International Conference on Intelligent Robots and Systems*, 2013, pp. 5134–5140
66. B.R. Whittington, D.G. Thelen, A simple mass-spring model with roller feet can induce the ground reactions observed in human walking. J. Biomech. Eng. **131**, 011013 (2009)
67. A. Wu, H. Geyer, The 3-D spring-mass model reveals a time-based deadbeat control for highly robust running and steering in uncertain environments. IEEE Trans. Robot. **29**(5), 1114–1124 (2013)
68. H. Yu, M. Li, H. Cai, Approximating the stance map of the SLIP runner based on perturbation approach, in *Proceedings of IEEE International Conference on Robotics and Automation*, 2012, pp. 4197–4203
69. G. Zeglin, *The Bow Leg Hopping Robot*, Ph.D., CMU-RI-TR-99-33, Carnegie Mellon University, 1999